Tonal active control of the power scattered by locally-reacting spheres using a small number of radiators near the surface

Mihai ORITA[1]; Stephen ELLIOTT[2]; Jordan CHEER[3]

[1, 2, 3] Institute of Sound and Vibration Research, United Kingdom

ABSTRACT

A theoretical investigation is performed where spherical harmonic series expansions are used to describe the primary and secondary pressure fields in the problem of actively controlling sound scattering around spheres. The study focuses on the scenario of point-monopoles radiators in the vicinity of a sphere with a uniform, locally-reacting and real-valued surface impedance. A control method based on minimizing the contributions of the spherical harmonic components to the scattered sound power is proposed. Under the established circumstances, any radiated sound power is found to be dominated by a few spherical harmonic terms of low degree in the region of large relative wavelength. As this wavelength decreases, numerous terms of higher degree become significant, thus increasingly more sources are required to achieve any suppression. A study case is performed where one point-monopole is placed at infinite distance to form an incident plane-wave. The scattering due to this is controlled with up to four point-monopoles on or near the surface of the sphere. Progressively better attenuation is achieved at large relative wavelength when increasing the number of control sources and the behaviour can be described using asymptotes of the spherical harmonic coefficients.

Keywords: Active Control, Sound Scattering, Spherical Harmonics

1. INTRODUCTION

Scattering represents the behaviour generated in the medium surrounding an obstacle when the combination of travelling waves forming a disturbance impinges on it. This behaviour is the total result of reflection, absorption and diffraction. In the case of acoustic waves, the understanding and control of scattering is important for a number of applications. One such example is binaural sound reproduction where the physical presence of the head plays a major role on the perceived sound [1]. Another example is acoustic cloaking, which has its purpose in situations where it is complicated to achieve desirable sound properties of certain elements. Structural components such as walls, columns, rafters and balconies have an impact on the soundscape within a building [2]. The ability to acoustically hide these once constructed could potentially simplify some of the challenges in designing spaces within concert halls, schools and hospitals that require specific acoustic properties.

In general, traditional passive absorption has drawbacks when it comes to performance and covered frequency range, which has sparked research interest into alternatives such as active control [3, 4]. When it comes to actively controlling sound scattering, there are currently two fundamental strategies. The first is a theoretical approach based on surrounding the obstacle with continuous layers of sensors and actuators in order to achieve perfect cancellation [5, 6]. The second method is rooted in practical realization and relies on supressing the scattered field, for a given frequency, by minimizing its radiated power at a finite number of error sensor positions with a finite number of control actuators [7-9]. In some of these works, the sound fields are modelled as series of orthogonal basis functions, i.e. expansions into uncoupled components that can be individually studied and manipulated. However, this quality can be further exploited when deriving the optimal strengths of the control sources.

The current paper proposes and theoretically investigates an alternative to the second fundamental strategy described above. This is done in the rudimentary case of an absorptive model for a spherical scatterer, surrounded by point-monopole sources, and consists of minimizing the contributions to the scattered sound power of the spherical harmonic components rather than the pressure at error points.

---

[1] Mihai.Orita@soton.ac.uk
[2] S.J.Elliott@soton.ac.uk
[3] J.Cheer@soton.ac.uk

2. THEORETICAL BACKGROUND

2.1 Spherical Harmonic Representations for Sound Scattering from Spheres

Let there be a fluid that is stationary, isentropic, inviscid and a perfect gas. The motion of acoustic waves propagating through this medium is governed by the linearized wave equation in the time domain. Given a system of spherical polar coordinates, as defined in [10], the equation can be solved to yield the general solution for the complex-valued acoustic pressure at location (r, θ, φ) [10, 11]

$$p(r,\theta,\varphi) = \sum_{n=0}^{\infty} \sum_{m=-n}^{n} U_{n,m} j_n(kr) Y_{n,m}^{(\mathbb{R})}(\theta,\varphi) + \sum_{n=0}^{\infty} \sum_{m=-n}^{n} V_{n,m} h_n(kr) Y_{n,m}^{(\mathbb{R})}(\theta,\varphi), \qquad (1)$$

at a single angular frequency ω. k represents the wavenumber associated with ω. A factor of $e^{j\omega t}$ is omitted in (1) for convenience of notation, and it represents the chosen time-frequency convention.

Expression (1) is composed of an interior solution, the first double summation, and an exterior one, the second double summation, which are distinct through their different regions of validity [10]. $j_n(kr)$ and $h_n(kr)$ are the spherical Bessel function of the first kind and, respectively, the spherical Hankel function of the second kind, as detailed in [10]. They describe the variation of the acoustic field with radial distance. The basis functions $Y_{n,m}^{(\mathbb{R})}(\theta,\varphi)$ are the real-valued spherical harmonics [11]

$$Y_{n,m}^{(\mathbb{R})}(\theta,\varphi) = \sqrt{\varepsilon_m/(4\pi)}\sqrt{(2n+1)(n-m)!/(n+m)!}\, P_n^m(\cos\theta)\, \mathrm{func}_m(m\varphi), \qquad (2)$$

where $\varepsilon_m = 2$ for $|m| \geq 1$ and $\varepsilon_0 = 1$, while $\mathrm{func}_{-|m|} = \sin$ and $\mathrm{func}_{|m|} = \cos$. $P_n^m(x)$ are the associated Legendre functions; however, they are defined as in [10], rather than in [11], to include the $(-1)^m$ factor corresponding to the Condon-Shortley phase. $Y_{n,m}^{(\mathbb{R})}(\theta,\varphi)$ can be interpreted as 3D patterns of angular variation around a given coordinate system and they can be visualized in [12]. $U_{n,m}$ and $V_{n,m}$ are complex-valued coefficients which uniquely define a particular sound field and are derived based on the circumstances of the given problem (e.g. boundary conditions on obstacles).

When it comes to the exterior solution in particular, the acoustic power it radiates is [10, 11]

$$W = \frac{1}{2\rho c k^2} \sum_{n=0}^{\infty} \sum_{m=-n}^{n} |V_{n,m}|^2. \qquad (3)$$

Each spherical harmonic component (n, m) contributes independently to the overall radiation and, thus, they are uncoupled from each other. This is a direct result of the basis functions being orthogonal and leads to theoretical and practical benefits, as will become apparent later in the study.

The acoustic scattering from a uniform, locally-reacting impedance sphere can be described in terms spherical harmonic components by applying the boundary condition

$$jkp(r,\theta,\varphi) - \zeta \partial p(r,\theta,\varphi)/\partial r = 0, \qquad (4)$$

to the general solution in (1). $\zeta = Z/(\rho c)$ is the surface impedance of the sphere normalised by the characteristic acoustic impedance of the medium exterior to it. This model represents an impedance that is manifested at each point of the boundary in the outgoing normal direction, independent of its value at all other points. Furthermore, it is considered that $\zeta \in \mathbb{R}^{\geq 0}$. A negative real part translates into the sphere creating additional energy, which is not generally encountered in the natural world.

In the case of a monochromatic point-monopole, when placed in free-field at (r', θ', φ') while having a volumetric strength q', it generates a sound pressure that is expanded as [10, 11]

$$p_i(r,\theta,\varphi) = q' k^2 \rho c \sum_{n=0}^{\infty} \sum_{m=-n}^{n} j_n(kr_<) h_n(kr_>) Y_{n,m}^{(\mathbb{R})}(\theta',\varphi') Y_{n,m}^{(\mathbb{R})}(\theta,\varphi), \qquad (5)$$

where $r_<$ is equal to $\min(r, r')$ and $r_>$ is equal to $\max(r, r')$. Due to linearity, the total pressure field p_t resulting from the interaction between the point-monopole and a spherical obstacle of radius a, centred at the origin, is the superposition between the incident field (5) and a scattered field p_s taking the form of the exterior solution from (1). At $r = a$, applying (4) to the total field leads to

$$p_t(r,\theta,\varphi) = \begin{cases} \sum_{n=0}^{\infty} \sum_{m=-n}^{n} q' k^2 \rho c [j_n(kr') - R_{\infty,n} h_n(kr')] Y_{n,m}^{(\mathbb{R})}(\theta',\varphi') h_n(kr) Y_{n,m}^{(\mathbb{R})}(\theta,\varphi), r > r' \\ \\ \sum_{n=0}^{\infty} \sum_{m=-n}^{n} q' k^2 \rho c [j_n(kr) - R_{\infty,n} h_n(kr)] h_n(kr') Y_{n,m}^{(\mathbb{R})}(\theta',\varphi') Y_{n,m}^{(\mathbb{R})}(\theta,\varphi), r < r' \end{cases}, \qquad (6)$$

and, by extension, to the scattered field

$$p_s(r,\theta,\varphi) = \sum_{n=0}^{\infty} \sum_{m=-n}^{n} -q'k^2\rho c R_{\infty,n} h_n(kr') Y_{n,m}^{(\mathbb{R})}(\theta',\varphi') \, h_n(kr) Y_{n,m}^{(\mathbb{R})}(\theta,\varphi) \, , \qquad (7)$$

where $R_{\infty,n} = [j_n(ka) + j\zeta j_n'(ka)]/[h_n(ka) + j\zeta h_n'(ka)]$. $j_n'(ka)$ and $h_n'(ka)$ are the first derivatives in respect to the dimensionless quantity ka, which describes the wavelength of sound relative to the size of the scatterer as an alternative to frequency. The scattered field (7) is present in both radial regions of (6) and is an exterior solution. The acoustic field generated directly by the point-monopole is converging towards the origin between r' and a, where it has the form of an interior solution, while diverging away from the origin after r', where it is an exterior solution.

Allowing $r' \to \infty$ in (6) imposes the first branch and results in the scattering of a plane-wave of magnitude P_i arriving from angles (θ',φ'), where the total and scattered pressure fields are [10, 11]

$$p_t(r,\theta,\varphi) = \sum_{n=0}^{\infty} \sum_{m=-n}^{n} 4\pi P_i j^n \big[j_n(kr) - R_{\infty,n} h_n(kr) \big] Y_{n,m}^{(\mathbb{R})}(\theta',\varphi') Y_{n,m}^{(\mathbb{R})}(\theta,\varphi) \, , \qquad (8)$$

$$p_s(r,\theta,\varphi) = \sum_{n=0}^{\infty} \sum_{m=-n}^{n} -4\pi P_i j^n R_{\infty,n} Y_{n,m}^{(\mathbb{R})}(\theta',\varphi') h_n(kr) Y_{n,m}^{(\mathbb{R})}(\theta,\varphi) \, . \qquad (9)$$

Furthermore, allowing $r' = a$ in (6) also imposes the first branch and yields the radiated pressure of a point-monopole with source strength q', situated on a spherical baffle at location (θ',φ') [10, 11]

$$p_r(r,\theta,\varphi) = \sum_{n=0}^{\infty} \sum_{m=-n}^{n} \frac{q'\rho c}{a^2} \frac{\zeta}{h_n(ka) + j\zeta h_n'(ka)} Y_{n,m}^{(\mathbb{R})}(\theta',\varphi') h_n(kr) Y_{n,m}^{(\mathbb{R})}(\theta,\varphi) \, . \qquad (10)$$

2.2 Tonal Active Control of Scattering Based on Spherical Harmonic Coefficients

When it comes to the problem of actively supressing the scattering around the sphere of radius a, let the primary field be the superposition of scattered fields due to F incident point-monopole disturbances, situated external to the obstacle. Each of these fields can take any of the forms expressed in (7), (9) or (10). In the same region of space, let there also be a secondary field composed of G point-monopole control sources, distinct from the previous set. Each of these fields can take the forms expressed in (6) or (10). It is chosen that the control system attenuates the radiated sound power of the primary, a measure that is invariant with space outside of the obstacle. When determining the sound power before and after control on a virtual sphere that encloses the G sources, all possible forms of acoustic field in the control problem are purely radiations, i.e. behave as exterior solutions.

The above tactic leads to the considered primary and secondary fields being

$$p_d(r,\theta,\varphi) = \sum_{f} \sum_{n,m} d_{n,m}^{(f)} h_n(kr) Y_{n,m}^{(\mathbb{R})}(\theta,\varphi) \, , \qquad f \in \{1, 2 \dots F\} \, , \qquad (11)$$

$$p_B(r,\theta,\varphi) = \sum_{g} \sum_{n,m} q_g B_{n,m}^{(g)} h_n(kr) Y_{n,m}^{(\mathbb{R})}(\theta,\varphi) \, , \qquad g \in \{1, 2 \dots G\} \, , \qquad (12)$$

where the double summations are denoted in a compact way. The possible forms taken by $d_{n,m}^{(f)}$ and $B_{n,m}^{(g)}$ are shown in Table 1 for different regimes of r', where $R_n(r') = (ka)^2 \big[j_n(kr') - R_{\infty,n} h_n(kr') \big]$ and $R_n(a) = (ka)^2 \big[j_n(ka) - R_{\infty,n} h_n(ka) \big] = \zeta/[h_n(ka) + j\zeta h_n'(ka)]$. The field after control is

$$p_e(r,\theta,\varphi) = \sum_{n,m} e_{n,m} h_n(kr) Y_{n,m}^{(\mathbb{R})}(\theta,\varphi) = \sum_{n,m} \left(\sum_{f} d_{n,m}^{(f)} + \sum_{g} q_g B_{n,m}^{(g)} \right) h_n(kr) Y_{n,m}^{(\mathbb{R})}(\theta,\varphi) \qquad (13)$$

and, from (3), radiates a sound power of

$$W_e = \frac{1}{2\rho c k^2} \sum_{n,m} |e_{n,m}|^2 = \frac{1}{2\rho c k^2} \sum_{n,m} \left| \sum_{f} d_{n,m}^{(f)} + \sum_{g} q_g B_{n,m}^{(g)} \right|^2 \qquad (14)$$

W_e is a g-dimensional, continuous, quadratic function with the source strengths q_g as variables. Active control is meant to find the set of q_g for which this function admits a minimum, if any. In practice, manipulating (13) and (14) requires the truncation of the infinite summation over n, turning them into numerical results. Let $N \geq 0$ be the truncation and let the spherical harmonic terms (n,m)

Table 1 – Possible forms of spherical harmonic coefficients in primary and secondary

	$d_{n,m}^{(f)}$	$B_{n,m}^{(g)}$
$r' = a$	$q_f \rho c a^{-2} R_n(a) Y_{n,m}^{(\mathbb{R})}(\theta_f, \varphi_f)$	$\rho c a^{-2} R_n(a) Y_{n,m}^{(\mathbb{R})}(\theta_g, \varphi_g)$
$r' > a$	$-q_f k^2 \rho c R_{\infty,n} h_n(kr') Y_{n,m}^{(\mathbb{R})}(\theta_f, \varphi_f)$	$\rho c a^{-2} R_n(r') Y_{n,m}^{(\mathbb{R})}(\theta_g, \varphi_g)$
$r' \to \infty$	$-4\pi P_f j^n R_{\infty,n} Y_{n,m}^{(\mathbb{R})}(\theta_f, \varphi_f)$	--

be arranged in the order: $(0,0)$, $(1,-1)$, $(1,0)$, $(1,1)$ ... $(N,-N)$ ... $(N,0)$... (N,N). This leads to a total of $L = (N+1)^2$ components present in the series, of which $2n+1$ are of the same degree n.

The version of (13) truncated to $n = N$ can be arranged into the matrix equation

$$\mathbf{e} = \mathbf{d} + \mathbf{B}\mathbf{q} . \tag{15}$$

The $L \times 1$ column vector $\mathbf{d}$ contains the components of the primary and is expressed as

$$\mathbf{d} = \left[\sum_f d_{0,0}^{(f)}, \sum_f d_{1,-1}^{(f)}, \sum_f d_{1,0}^{(f)}, \sum_f d_{1,1}^{(f)} \cdots \sum_f d_{N,-N}^{(f)} \cdots \sum_f d_{N,0}^{(f)} \cdots \sum_f d_{N,N}^{(f)} \right]^{\mathrm{T}} . \tag{16}$$

In the $L \times G$ matrix $\mathbf{B}$, the g-th column contains the corresponding components in the secondary for the g-th control source and is given by

$$\mathbf{B}_{*,g} = \left[B_{0,0}^{(g)}, B_{1,-1}^{(g)}, B_{1,0}^{(g)}, B_{1,1}^{(g)} \cdots B_{N,-N}^{(g)} \cdots B_{N,0}^{(g)} \cdots B_{N,N}^{(g)} \right]^{\mathrm{T}} . \tag{17}$$

The $G \times 1$ column vector $\mathbf{q}$ is governed by the constraint of the control problem and is equal to

$$\mathbf{q} = \left[q_1, q_2, q_3 \cdots q_g \right]^{\mathrm{T}} . \tag{18}$$

The $L \times 1$ column vector $\mathbf{e}$ contains the components after control is applied and is written as

$$\mathbf{e} = \left[e_{0,0}, e_{1,-1}, e_{1,0}, e_{1,1} \cdots e_{N,-N} \cdots e_{N,0} \cdots e_{N,N} \right]^{\mathrm{T}} . \tag{19}$$

Relation (15) forms a linear system of equations that is an established topic in the area of active control [3, 4]. The system emerges when using the traditional strategy of minimizing the means square pressures or particle velocities at a finite set of sensor positions, given a finite set of secondary sources. If (15) is overdetermined, i.e. $G < L$, and $\mathbf{B}^{\mathrm{H}}\mathbf{B}$ is positive-definite, then source strengths given by

$$\mathbf{q}_{opt} = -[\mathbf{B}^{\mathrm{H}}\mathbf{B}]^{-1}\mathbf{B}^{\mathrm{H}}\mathbf{d} \tag{20}$$

form the unique, optimal set that produces a minimum, if it exists, in the cost function

$$J = W_e = \mathbf{e}^{\mathrm{H}}\mathbf{e} = \sum_{n,m} |e_{n,m}|^2 \tag{21}$$

at a single value of ka. (21) is the truncated version of (14) without the factor of $1/(2\rho c k^2)$. This factor is a constant relative to ka and does not affect the derivation of $\mathbf{q}_{opt}$ from (20); however, it does scale the minimum achievable value of W_e. It can be concluded that minimizing either the mean squared pressures at sensing locations or the mean squared spherical harmonic coefficients of the pressure leads to the same analytical result for the scattered power after control. The two methods differ when it comes to inner and cross coupling of primary and secondary. For a grid of pressure sensors, the elements in $\mathbf{d}$ and, respectively, in each column of $\mathbf{B}$ are inherently interconnected, thus limiting the optimization. Spherical harmonic coefficients are uncoupled and do not exhibit this.

The amount of attenuation achievable after the optimization depends on which elements of $\mathbf{d}$ are dominant and on how well the corresponding elements of each row in $\mathbf{B}$ can couple into them. The act of altering or completely cancelling a specific spherical harmonic component in (15) establishes one constraint on the set of source strengths, thus creating residuals in the other non-zero components. The effect is referred to as spill-over [3, 4] and is unavoidable in the current model. This is because all forms of the primary and secondary described in Table 1 have at least a countably infinite set of non-zero spherical harmonic components, regardless of point-monopole location in the region $r \geq a$. Imposing specific behaviours on G distinct components requires at least G distinct sources.

While the problem is not ill-conditioned, the optimization balances between manipulating specific components and generating residuals, such that the passive situation is not made worse after control. However, (20) is a numerical result and cannot directly describe how each optimal variable is chosen.

Table 2 – Asymptotic behavior relative to ka of $R_n(r'_\tau)$ factors in spherical harmonic coefficients

	$ka \ll 1, n = 0$	$ka \ll n, n \geq 1$	$ka \to \infty$
$R_n(a)$	$(ka)^2 \dfrac{\zeta}{jka+\zeta}$	$\dfrac{2^{n-1}(n-1)!}{(2n-1)!}(ka)^{n+2}\dfrac{\zeta}{jka+\zeta(n+1)}$	$\dfrac{\zeta ka}{j^{n+1}e^{-jka}(1+\zeta)}$
$R_n(r')$	$(ka)^2\left[1-\dfrac{a}{r'}\dfrac{1-j\zeta ka/3}{1+\zeta/(jka)}\right]$	$\dfrac{(ka)^2(kr')^n}{(2n+1)!!}\left[1-j\left(\dfrac{a}{r'}\right)^{2n+1}\dfrac{ka+j\zeta n}{jka+\zeta(n+1)}\right]$	$\dfrac{(ka)^2}{(kr')}\left[\sin\left(kr'-\dfrac{n\pi}{2}\right)-\dfrac{e^{-jk(r'-a)}\mathcal{F}}{(1+\zeta)}\right]$
$R_{\infty,n}$	$(ka)^2\dfrac{1-j\zeta ka/3}{jka+\zeta}$	$\left[\dfrac{2^n n!}{(2n)!}\right]^2\dfrac{(ka)^{2n+1}}{(2n+1)}\dfrac{ka+j\zeta n}{jka+\zeta(n+1)}$	$\dfrac{\mathcal{F}}{j^{n+1}e^{-jka}(1+\zeta)}$

2.3 Method for Assessing the Performance of Active Control

To interpret the outcome of (20), the spherical harmonic coefficients after control are compared to analytical predictions. These require studying the behaviour of the coefficients in the primary and secondary. The forms of $d_{n,m}^{(f)}$ and $B_{n,m}^{(g)}$ from Table 1 share a general structure of three factors

$$\tau_{n,m} = \mathfrak{C}_{\tau,n}R_n(r'_\tau)Y_{n,m}^{(\mathbb{R})}(\theta_\tau, \varphi_\tau). \tag{22}$$

Relative to ka, $\mathfrak{C}_{\tau,n}$ is either a real or purely imaginary constant that gives the units of $\tau_{n,m}$. $R_n(r'_\tau)$ is a dimensionless, complex-valued quantity. It solely governs the variation with ka of $\tau_{n,m}$ and, hence, that of the contribution to the radiated sound power, before and after control, from the spherical harmonic terms of degree n. $Y_{n,m}^{(\mathbb{R})}(\theta_\tau, \varphi_\tau)$ is a real-valued, dimensionless constant relative to ka. When using the general form (22) into (3), the spherical harmonics closure relation reduces (3) to

$$W_\tau = \frac{1}{2\rho ck^2}\sum_{n,m}|\tau_{n,m}|^2 = \frac{a^2}{8\pi\rho c}\sum_n (2n+1)|\mathfrak{C}_{\tau,n}|^2|R_n(r'_\tau)|^2/(ka)^2 = \sum_n W_{\tau,n}, \tag{23}$$

where $W_{\tau,n}$ is the combined contribution to the radiated power of components with degree n.

In (23), $|\mathfrak{C}_{\tau,n}|$ does not depend on n, given the results from Table 1. The asymptotic behaviour of the $R_n(r'_\tau)$ factors when ka becomes very small or very large can be established, as seen in [13, 14]. Choosing the appropriate expansion for the spherical Bessel and Hankel functions that compose $R_n(r'_\tau)$ and then considering the leading order term, yields the results from Table 2, where $\mathcal{F} = \sin(ka - n\pi/2) + j\zeta\cos(ka - n\pi/2)$. Computing these results for different values of n and using them to analyse $W_{\tau,n}$ reveals that, in the region of $ka \ll 1$, the contribution of a lower n component is larger than that of a higher n one while, generally, also varying as a lower power of ka. This leads to the radiated power being dominated by the first few spherical harmonic components. Furthermore, at large ka, W_τ is dominated by a number of spherical harmonic components of high n.

As ka increases, achieving considerable suppression of the scattered power implies more control sources, such that each component that becomes significant can be addressed. Thus, when using a small number of sources, the predicting the asymptotes when $ka \ll 1$ is of interest in the analysis.

3. STUDY CASE: ACTIVE CONTROL OF SINGLE PLANE-WAVE SCATTERING

3.1 Defining the Active Control Problem

The specific example presented in this paper consists of controlling the scattering of a single monochromatic plane-wave as it insonifies the impedance sphere. The plane-wave has a magnitude $P_i = 1$ Pa and arrives from the incidence angles (θ_i, φ_i). The generated scattered field represents the primary and is expressed as (9), with coefficients given by $d_{n,m} = -4\pi P_i j^n R_{\infty,n}Y_{n,m}^{(\mathbb{R})}(\theta_i, \varphi_i)$. The plane-wave is chosen to propagate parallel to the yz-plane, in the direction of the z-axis from $-\infty$ to ∞. This corresponds to $(\theta_i, \varphi_i) = (\pi, \pi/2)$ and, from (2), results in only the components of order $m = 0$ being activated in the primary. Furthermore, three spheres of surface impedances $\zeta = 0.01$, $\zeta = 1$ and $\zeta = 100$ are exemplified. The first and the last cases approximate a soft sphere of $\zeta = 0$ and, respectively, a hard sphere of $\zeta = \infty$. This was done to maintain consistency, as a secondary source on the surface of a soft obstacle cannot radiate. The case of $\zeta = 1$ represents the impedance of the sphere matched to that of the surrounding medium. Air at normal atmospheric conditions is used in all results.

The scattered power due to the plane-wave, W_d, is expressed using the coefficients $d_{n,m}$ in (3). This is normalized by the power associated with the plane-wave, $W_i = \pi a^2 P_i^2/(2\rho c)$, then plotted as $\Pi_d = W_d/W_i$ versus ka for the three cases of impedance in the graphs of Figure 1. A truncation degree of $N = 100$ was used alongside a range of 1001 logarithmically-spaced points between $ka = 0.1$ and $ka = 100$. Simulations have shown that, at a given large value of ka, the number of spherical harmonic degrees n that contribute significantly to this scattered power is equal to ka.

The asymptotic behaviour of Π_d when $ka \ll 1$ is dictated by the most dominant spherical harmonic terms in that region, which can be established from Table 2. The $\zeta = 0.01$ and $\zeta = 1$ spheres are both dominated by the $(n,m) = (0,0)$ term, which leads to their normalized powers having asymptotes of 4 and, respectively, $4(ka)^2$. The $\zeta = 100$ sphere is dominated by both $(n,m) = (0,0)$ and $(n,m) = (1,0)$ terms, which contribute to the scattered power as $4(ka)^4/9$ and, respectively, $3(ka)^4/9$. This leads to an asymptote of Π_d equal to $7(ka)^4/9$, as described in [15].

In the following paragraphs, results of active control are shown for the four different arrangements of point-monopole sources depicted in the diagram of Figure 1. To have corresponding spherical harmonic components activated in both primary and secondary, the sources are placed on the z-axis.

3.2 Control Results when Using a Small Number of Surface Radiators

A secondary field composed of point-monopoles on the scattering surface has the coefficients $B_{n,m}^{(g)} = \rho c a^{-2} R_n(a) Y_{n,m}^{(\mathbb{R})}(\theta_g, \varphi_g)$. Simulations show that the power radiated by such a field follows the same truncation rule as the primary, where $N = ka$ terms are required at a given large value of ka.

Choosing the same truncation degree, $N = 100$, for both primary and secondary, the minimization (20) was computed over the $N + 1$ contributing spherical harmonic components of $m = 0$, at each 1001 logarithmically-spaced points between $ka = 0.1$ and $ka = 100$. For a single control source placed at $(\theta_1, \varphi_1) = (0,0)$, it is assumed that the minimization attempts to perfectly cancel the $(n,m) = (0,0)$ term, which is the largest for all three cases of ζ. Then, the optimal source strength is

$$q_1 = -d_{0,0}/B_{0,0} = 4\pi P_i a^2 (\rho c)^{-1} R_{\infty,0}/R_0(a),\tag{24}$$

and, after control, the $(n,m) = (1,0)$ term is

$$e_{1,0} = d_{1,0} - d_{0,0} B_{1,0}/B_{0,0} = 2\sqrt{3\pi} P_i \left[-jR_{\infty,1} + R_{\infty,0} R_1(a)/R_0(a)\right].\tag{25}$$

The formulas from Table 2 are used in (24) and (25) to calculate the asymptotic behaviour after control when $ka \ll 1$. The hierarchy between contributions to the power is maintained, ignoring the cancelled component. The $(n,m) = (1,0)$ term varies as the lowest power of ka and, thus, is the new dominant component. This translates into the normalized scattered power after control, $\Pi_e = W_e/W_i$, having asymptotes of $12(ka)^2$, $4(ka)^4/3$ and $3(ka)^4/9$ for $\zeta = 0.01$, $\zeta = 1$ and, respectively, $\zeta = 100$.
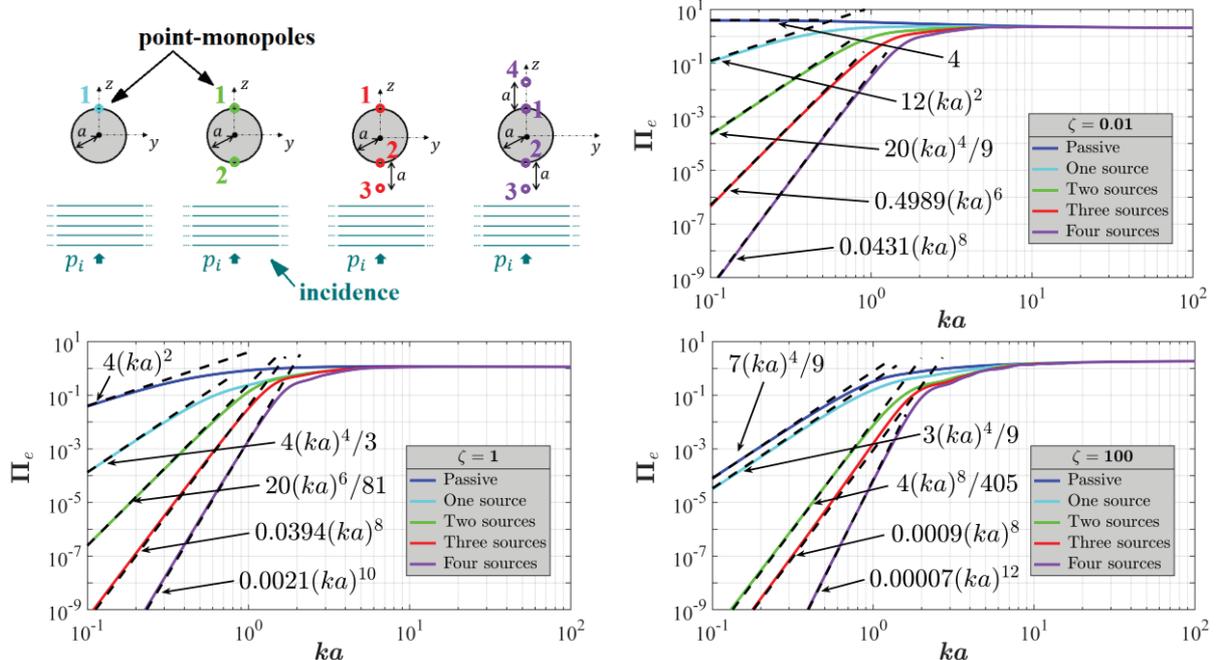

Figure 1 – Normalized scattered power due to plane-wave before and after control, as a function of ka

A second point-monopole is now placed on the surface of the sphere at $(\theta_2, \varphi_2) = (\pi, \pi/2)$ and all the computational circumstances are maintained. It is assumed the minimization attempts to perfectly supress both the $(n, m) = (0,0)$ and $(n, m) = (1,0)$ terms, which are the largest two for all three cases of ζ. Due to the parity of the spherical harmonic functions, the linear combinations

$$q_1 + q_2 = -d_{0,0}/B_{0,0}^{(2)} = 4\pi P_i a^2 (\rho c)^{-1} R_{\infty,0}/R_0(a) , \qquad (26)$$

$$q_2 - q_1 = -d_{1,0}/B_{1,0}^{(2)} = 4\pi j P_i a^2 (\rho c)^{-1} R_{\infty,1}/R_1(a) , \qquad (27)$$

of the two optimal source strengths govern (15). After control, the $(n, m) = (2,0)$ term is expressed as

$$e_{2,0} = d_{2,0} - d_{0,0} B_{2,0}^{(2)}/B_{0,0}^{(2)} = 2\sqrt{5\pi} P_i \left[R_{\infty,2} + R_{\infty,0} R_2(a)/R_0(a) \right] \qquad (28)$$

and is now the dominant component in the $ka \ll 1$ region, yielding asymptotes of Π_e equal to $20(ka)^4/9$, $20(ka)^6/81$ and $4(ka)^8/405$ for $\zeta = 0.01$, $\zeta = 1$ and, respectively, $\zeta = 100$.

For both control arrangements, the predicted asymptotes, seen as dashed lines in Figure 1, are good representations of the computed outcomes of (20), seen as solid coloured lines in Figure 1. Overall, the reduction of Π_e has improved when going from one to two sources. For $\zeta = 100$, considerably better attenuation is achieved with two sources as both significant terms in the primary are addressed.

3.3 Control Results when Using a Small Number of Surface and Near-Surface Radiators

To control more than the first two spherical harmonic components, extra variables need to be introduced in (15). However, new sources have to be placed such that their coefficients $B_{n,m}^{(g)}$ are considerably different from $B_{n,m}^{(1)}$ and $B_{n,m}^{(2)}$ used previously. Otherwise, the control generates as much attenuation of the power as for the previous two sources and manifests ill-conditioning when inverting $\mathbf{B}^H \mathbf{B}$. Therefore, extra point-monopoles are placed away from the surface of the scatterer at a distance of $r' = 2a$. In this way, the secondary has $B_{n,m}^{(g)}$ coefficients that can have either of the two forms from Table 1. Simulations show that the power radiated by such a secondary requires a truncation degree of $N = kr'$, at a given large value of ka, where r' corresponds to the source furthest away.

In the previous arrangement of two control sources, a third point-monopole is now added at $(r_3', \theta_3, \varphi_3) = (2a, \pi, \pi/2)$. (20) is computed under the same circumstances, but the higher truncation degree corresponding to the secondary, $N = 200$, is chosen rather than that of the primary to avoid aliasing. This mismatch introduces terms of high degree n that are zero in the primary but non-zero in the secondary. Attenuation is achieved only in the $ka \ll 1$ region, which is dominated by terms of low degree n and, hence, is minimally affected by the mismatch. Assuming that the spherical harmonic components of the first three degrees n are perfectly cancelled leads to the optimal source strengths

$$q_1 + q_2 = -d_{0,0}/B_{0,0}^{(2)} - \left(d_{2,0} B_{0,0}^{(2)} B_{0,0}^{(3)} - d_{0,0} B_{2,0}^{(2)} B_{0,0}^{(3)} \right) / \left(B_{2,0}^{(2)} B_{0,0}^{(3)} B_{0,0}^{(2)} - B_{0,0}^{(2)} B_{2,0}^{(3)} B_{0,0}^{(2)} \right), \qquad (29)$$

$$q_2 - q_1 = -d_{1,0}/B_{1,0}^{(2)} - \left(d_{2,0} B_{0,0}^{(2)} B_{1,0}^{(3)} - d_{0,0} B_{2,0}^{(2)} B_{1,0}^{(3)} \right) / \left(B_{2,0}^{(2)} B_{0,0}^{(3)} B_{1,0}^{(2)} - B_{0,0}^{(2)} B_{2,0}^{(3)} B_{1,0}^{(2)} \right), \qquad (30)$$

$$q_3 = \left(d_{2,0} B_{0,0}^{(2)} - d_{0,0} B_{2,0}^{(2)} \right) / \left(B_{2,0}^{(2)} B_{0,0}^{(3)} - B_{0,0}^{(2)} B_{2,0}^{(3)} \right), \qquad (31)$$

that govern the individual equations of (15). After control, the $(n, m) = (3,0)$ term is expressed as

$$e_{3,0} = d_{3,0} - d_{1,0} B_{3,0}^{(2)}/B_{1,0}^{(2)} + \left(B_{3,0}^{(3)} - B_{1,0}^{(3)}/B_{1,0}^{(2)} \right) \left(d_{2,0} B_{0,0}^{(2)} - d_{0,0} B_{2,0}^{(2)} \right) / \left(B_{2,0}^{(2)} B_{0,0}^{(3)} - B_{0,0}^{(2)} B_{2,0}^{(3)} \right) \qquad (32)$$

and now dominates in the $ka \ll 1$ region, yielding asymptotes of Π_e equal to $0.4989(ka)^6$, $0.0394(ka)^8$ and $0.0009(ka)^8$ for $\zeta = 0.01$, $\zeta = 1$ and, respectively, $\zeta = 100$.

Lastly, a fourth source is now placed at $(r_4', \theta_4, \varphi_4) = (2a, 0,0)$. The previous computational context is maintained. Assuming that the components of first four degrees n are perfectly cancelled yields

$$q_1 + q_2 = \left(d_{2,0} B_{0,0}^{(3)} - d_{0,0} B_{2,0}^{(3)} \right) / \left(B_{0,0}^{(2)} B_{2,0}^{(3)} - B_{2,0}^{(2)} B_{0,0}^{(3)} \right), \qquad (33)$$

$$q_2 - q_1 = \left(d_{3,0} B_{1,0}^{(3)} - d_{1,0} B_{3,0}^{(3)} \right) / \left(B_{1,0}^{(2)} B_{3,0}^{(3)} - B_{3,0}^{(2)} B_{1,0}^{(3)} \right), \qquad (34)$$

$$q_3 + q_4 = \left(d_{2,0} B_{0,0}^{(2)} - d_{0,0} B_{2,0}^{(2)} \right) / \left(B_{2,0}^{(2)} B_{0,0}^{(3)} - B_{0,0}^{(2)} B_{2,0}^{(3)} \right), \qquad (35)$$

$$q_3 - q_4 = \left(d_{3,0} B_{1,0}^{(2)} - d_{1,0} B_{3,0}^{(2)} \right) / \left(B_{3,0}^{(2)} B_{1,0}^{(3)} - B_{1,0}^{(2)} B_{3,0}^{(3)} \right), \qquad (36)$$

which govern the individual equations in (15). After control, the $(n, m) = (4,0)$ term becomes

$$e_{4,0} = d_{4,0} + \left[d_{0,0} \left(B_{4,0}^{(3)} B_{2,0}^{(2)} - B_{4,0}^{(2)} B_{2,0}^{(3)} \right) + d_{2,0} \left(B_{4,0}^{(2)} B_{0,0}^{(3)} - B_{4,0}^{(3)} B_{0,0}^{(2)} \right) \right] / \left(B_{0,0}^{(2)} B_{2,0}^{(3)} - B_{2,0}^{(2)} B_{0,0}^{(3)} \right) \quad (37)$$

and now dominates in the $ka \ll 1$ region, yielding asymptotes of Π_e equal to $0.0431(ka)^8$, $0.0021(ka)^{10}$ and $0.00007(ka)^{12}$ for $\zeta = 0.01$, $\zeta = 1$ and, respectively, $\zeta = 100$.

For the current two control arrangements, the predicted asymptotes, seen as dashed lines in Figure 1, are also good representations of the computed outcomes of (20), seen as solid coloured lines in Figure 1. Going from two to three to four sources progressively improves the obtained suppression at low ka. The amount is different between cases of ζ, as their corresponding asymptotes are dissimilar.

4. CONCLUSIONS

A theoretical investigation has been realized where spherical harmonic expansions were used to describe the primary and secondary fields, as well as the minimization method, in the problem of actively controlling the sound scattering from a sphere. Simulations were performed for truncated versions of these expansions, in the case of a single plane-wave arriving onto a uniform, locally-reacting sphere. A small number of point-monopoles on and near the surface of the obstacle were ideally placed relative to the known incidence. In the Rayleigh region, the spherical harmonic coefficients in both primary and secondary form a hierarchy of ascending powers of ka with increasing n. Thus, progressively better attenuation of the scattered power was achieved when adding a few more sources, as more of the first dominant components in the hierarchy can be controlled. This behavior was analytically predicted using the asymptotes of the spherical harmonic coefficients.

In terms of future work, the presented modelling and control strategies can be extended to scenarios beyond that of a single plane-wave. Also, characterizing the effects on control performance of using a large number of sources and of solely moving the sources away from the obstacle can be further explored. In terms of experimental validation, a necessary first step is to devise a practical active control system that can sense and manipulate a 3D sound field as spherical harmonic components.

ACKNOWLEDGEMENTS

REFERENCES

1. Duda RO, Martens WL. Range dependence of the response of a spherical head model. J Acoust Soc Am. 1998;104(5):3048-58.
2. Kuttruff H. Room Acoustics. 5th ed. New York, USA: Taylor & Francis; 2009.
3. Nelson PA, Elliott SJ. Active Control of Sound. London, UK: Academic press; 1991.
4. Fuller CC, Elliott S, Nelson PA. Active Control of Vibration. London, UK: Academic Press; 1996.
5. Guevara Vasquez F, Milton G, Onofrei D. Exterior cloaking with active sources in two dimensional acoustics. Wave Motion. 2011;48(6):515-24.
6. Norris AN, Amirkulova FA, Parnell WJ. Source amplitudes for active exterior cloaking. Inverse Problems. 2012;28(10).
7. Friot E, Guillermin R, Winninger M. Active control of scattered acoustic radiation: a real-time implementation for a three-dimensional object. Acta Acustica united with Acustica. 2006;92(2):278-88.
8. Cheer J. Active control of scattered acoustic fields: Cancellation, reproduction and cloaking. The Journal of the Acoustical Society of America. 2016;140(3):1502-12.
9. Liu J, Wang X, Wu M, Yang J. An active control strategy for the scattered sound field control of a rigid sphere. J Acoust Soc Am. 2018;144(1):EL52-EL8.
10. Williams EG. Chapter 6 - Spherical Waves. In: Williams EG, editor. Fourier Acoustics. London: Academic Press; 1999. p. 183-234.
11. Poletti MA. Unified description of Ambisonics using real and complex spherical harmonics. Ambisonics Symposium 2009; 25-27 June 2009; Graz, Austria2009.
12. Green R. Spherical harmonic lighting: the gritty details. Game Developers Conference; 2003.
13. Godin OA. Rayleigh scattering of a spherical sound wave. J Acoust Soc Am. 2013;133(2):709-20.
14. Arfken GB, Weber HJ, Harris FE. Chapter 14 - Bessel Functions. In: Arfken GB, Weber HJ, Harris FE, editors. Mathematical Methods for Physicists 7th ed. Boston: Academic Press; 2013. p. 643-713.
15. Lamb H. Chapter VIII - Simple harmonic waves. Diffraction. In: Lamb H, editor. The Dynamical Theory of Sound. London, UK: E. Arnold; 1925. p. 223-53.